

A variational Bayesian spatial interaction model for estimating revenue and demand at business facilities

Shanaka Perera

University of Warwick, Coventry, United Kingdom

E-mail: s.perera@warwick.ac.uk[†]

Virginia Aglietti

University of Warwick, Coventry, United Kingdom

The Alan Turing Institute, London, United Kingdom

Theodoros Damoulas

University of Warwick, Coventry, United Kingdom

The Alan Turing Institute, London, United Kingdom

Summary. We study the problem of estimating potential revenue or demand at business facilities and understanding its generating mechanism. This problem arises in different fields such as operation research or urban science, and more generally, it is crucial for businesses' planning and decision making. We develop a Bayesian spatial interaction model, henceforth BSIM, which provides probabilistic predictions about revenues generated by a particular business location provided their features and the potential customers' characteristics in a given region. BSIM explicitly accounts for the competition among the competitive facilities through a probability value determined by evaluating a store-specific Gaussian distribution at a given customer location. We propose a scalable variational inference framework that, while being significantly faster than competing Markov Chain Monte Carlo inference schemes, exhibits comparable performances in terms of parameters identification and uncertainty quantification. We demonstrate the benefits of BSIM in various synthetic settings characterised by an increasing number of stores and customers. Finally, we construct a real-world, large spatial dataset for pub activities in London, UK, which includes over 1,500 pubs and 150,000 customer regions. We demonstrate how BSIM outperforms competing approaches on this large dataset in terms of prediction performances while providing results that are both interpretable and consistent with related indicators observed for the London region.

Keywords: Bayesian model; Markov Chain Monte Carlo; Spatial data; Spatial interaction model; Variational Inference

[†]*Address for correspondence:* Shanaka Perera, Department of Computer Science, University of Warwick, CV4 7AL, UK.

1. Introduction

Understanding the interaction between business facilities and consumer preferences is a prime factor of success for industries such as retail, healthcare and hospitality. Therefore, accurate predictions of potential sales at business locations are becoming crucial for planning and decision-making in the current ecosystem. Indeed, the continuous growth in e-commerce (ONS, 2020) is threatening the existence of traditional retail stores. We propose a Bayesian statistical methodology that, by capturing the relationship between attractiveness of the facility, distance between a business location and its customers, and demand in terms of buying power, allows to make probabilistic forecasts about potential revenue at a business facility while quantifying the uncertainty in these estimates.

One of the earliest statistical models of customer behaviors when choosing shopping facilities is a spatial interaction model, called Law of Retail Gravitation (Reilly et al., 1929), which was inspired by the Newtonian gravity model and formulated a customer’s choice between two facilities as a function of their attractiveness and distances. Huff (1963) subsequently extended this model to consider multiple facilities while providing a probabilistic interpretation for the spatial interactions between customers and facilities. In the following years, the Huff model (Huff, 1963) was improved by replacing the single attractiveness term determined by floorspace with a composite index of a set of attributes at the facility, including economic and structural factors (Nakanishi and Cooper, 1974; De Giovanni and Tadei, 2014). Most of the literature estimates the parameters of spatial interaction models by resorting to regression methods (Nakanishi and Cooper, 1974; Fotheringham and Webber, 1980; Li and Liu, 2012; Bektı et al., 2018) or by maximising the entropy with respect to some constraints (Fotheringham, 1983; Wilson, 2010). More recently, computationally intensive Markov Chain Monte Carlo (MCMC) schemes have been proposed as an alternative inference method within the Bayesian framework for modelling origin-destination flows but do not offer capabilities in estimating total revenue or demand generated at the destination (Ellam et al., 2018; Congdon, 2010; LeSage and Fischer, 2008).

Inspired by the literature on gravity models, we develop a Bayesian spatial interaction model, henceforth named BSIM, which provides probabilistic predictions about revenues generated at business facilities given their features and the potential customers’ characteristics in a specified region in space. We model the probability of a customer visiting each facility in a region through Gaussian densities in geographic space. Specifically, each density is centered on a facility with variance that is further determined by its attractiveness which in turn modelled as a function of internal and external characteristics (e.g. floorspace, distance to public transport access points) and customer perspective (e.g. customer rating). The revenues for each facility are then obtained by combining the probability of a customer visit with a proxy of the individuals buying power, which we assume to be a function of their socio-demographic characteristics. We adopt a Bayesian approach that enables us to adequately account for the uncertainty associated with the customer interactions with the facilities. Our framework not only gives accurate predictions but produces

interpretable results that can support experts’ decision-making processes. Moreover, this approach allows us to infer quantities at the business facility or customer level, such as revenue flow from customers to businesses. In BSIM, the posterior distributions of interest are intractable, and their approximation poses significant computational challenges. We address this issue by resorting to variational inference while also comparing with MCMC approximation. We demonstrate how our variational scheme is significantly faster compared to MCMC used in the literature while providing comparable results in terms of parameter identification and uncertainty quantification.

In the literature, experiments on spatial interaction modelling are limited to small synthetic datasets or real-world aggregated data since acquiring granular level real-world data is usually expensive (Berman and Krass, 2002; Aboolian et al., 2007). To address these constraints, we create a dataset that includes variables observed at a granular level for public houses (pubs) and customers. This is performed by combining large geospatial and non-geospatial data using open and commercial data sources. Additionally, we gather customer reviews from Google’s customer rating API, which covers a broader audience compared to the traditional survey methods found in the literature (Drezner, 2006). We demonstrate the benefits of the proposed methodology on this real-world large scale dataset and show how BSIM outperforms competing approaches in terms of prediction performances. Furthermore, we illustrate how BSIM provides interpretable results consistent with other industry-related indicators observed for London.

Our main contributions are: (a) we develop a Bayesian spatial interaction model (BSIM) that can be used to make probabilistic predictions of revenues or demand generated at business facilities and formulates the relationship between distance and attractiveness of facilities jointly, using a facility-specific probability distribution; (b) we propose a scalable variational inference and demonstrate its benefits compared to MCMC methods in a variety of experimental settings; (c) we construct an unprecedented real-world large spatial dataset for pub activities at the most granular level along with customer characteristics at the postcode level, collated from multiple sources; and (d) We show that our method provides the best predictive performance compared to competing approaches while providing inference at the level of customers and business facilities, delivering invaluable insights for planning and decision making. To the best of our knowledge, we are the first to demonstrate an application of a Bayesian spatial interactions model on a large scale real-world dataset describing pub activities in the Greater London area with more than 1,500 business locations and 150,000 customer regions.

This paper is organised as follows. In Section 2, we introduce BSIM and the related inference scheme. Then, we evaluate the model performance using synthetic experiments in Section 3. In Section 4, we introduce a comprehensive spatial database. Next, in Section 5, using the new dataset, we demonstrate the benefits of our approach by inferring the model parameters for a real-world case study. Finally, conclusions and future research directions are discussed in Section 6.

2. Methodology

We consider a regression problem for a given dataset $\mathcal{D} = \{\mathbf{x}_s, y_s\}_{s=1}^S$, where $\mathbf{x}_s \in \mathbb{R}^D$ represents the s -th store’s features and $y_s \in \mathbb{R}$ gives the revenue for the s -th store in a bounded region τ . Each feature vector $\mathbf{x}_s^\top = [\mathbf{1}_s^\top, \boldsymbol{\phi}_s^\top]$ includes the store location, which we denote by $\mathbf{l}_s \in \mathbb{R}^2$, and additional store characteristics denoted by $\boldsymbol{\phi}_s \in \mathbb{R}^{D-2}$, e.g. floor size. For notational convenience we will denote $S \times (D - 2)$ matrix of all stores characteristics by $\boldsymbol{\Phi}$. We assume the existence of N customers within τ where \mathbf{v}_n is the n -th row of $\mathbf{V} \in \mathbb{R}^{N \times P}$ and represents the features of the n -th customer. \mathbf{v}_n includes the customer location, which we denote by $\mathbf{m}_n \in \mathbb{R}^2$ and its characteristics such as income level.

2.1. Model Formulation

The proposed Bayesian Spatial Interaction Model (BSIM) is characterised by S Gaussian distributions, one for each store, which are uncorrelated a priori. Each Gaussian distribution, henceforth $\mathbf{Z}_s \sim \mathcal{N}(\boldsymbol{\mu}_s, \boldsymbol{\Sigma}_s)$, is centered on a store’s location $\boldsymbol{\mu}_s = \mathbf{l}_s$ and has a diagonal covariance matrix $\boldsymbol{\Sigma}_s = \sigma_s^2 \mathbf{I}$. The variance σ_s^2 captures level of “attraction” of a customer to a store. We propose two different alternative models for variance. In the first model σ_s^2 is written as a function of store specific coefficient $v_s \in \mathbb{R}$ that is:

$$\sigma_s^2 = \exp(v_s), \quad (1)$$

In the second, we improve the specifications by denoting v_s as a function of store characteristics:

$$v_s = \boldsymbol{\lambda}^\top \boldsymbol{\phi}_s + \varepsilon_s, \quad (2)$$

where $\boldsymbol{\lambda} \in \mathbb{R}^{D-2}$ represents a shared coefficients across the stores and ε_s denotes the unobservable store characteristics. Evaluating the probability density function (PDF) of the variable \mathbf{Z}_s at \mathbf{m}_n , which we denote by $\mathbf{Z}_s(\mathbf{m}_n)$, allows us to capture the likelihood for the n -th customer to visit the s -th store based on their distance and on the store characteristics. For illustration purposes, consider three stores where each has a Gaussian distribution centred on the store, as shown in Fig. 1.

Irrespective of the store’s attractiveness, customer behaviour is not affected after a certain maximum distance to the store, known as “consideration set” in marketing. Therefore, we truncate the Gaussian distributions in BSIM and force their densities to be zero beyond a given distance d_T from the store location. The truncated Gaussian PDF is given by:

$$\mathbf{Z}_s(\mathbf{m}_n) = \begin{cases} \frac{\exp(-d_{ns}^2/2\sigma_s^2)}{2\pi\sigma_s^2(1 - \exp(-d_T^2/2\sigma_s^2))}, & 0 \leq d_{ns} \leq d_T, \\ 0, & \text{otherwise,} \end{cases} \quad (3)$$

where d_{ns} denotes the Euclidean distance between the store and customer $d_{ns} = \|\mathbf{m}_n - \mathbf{l}_s\|_2$; see Appendix A for details. Fig. 2 demonstrates the truncated Gaussian densities corresponding to the distributions shown in Fig. 1.

‡We present the rest of the model in relation to the specific instantiation where a business location is a store, but this can be extended to other business facilities.

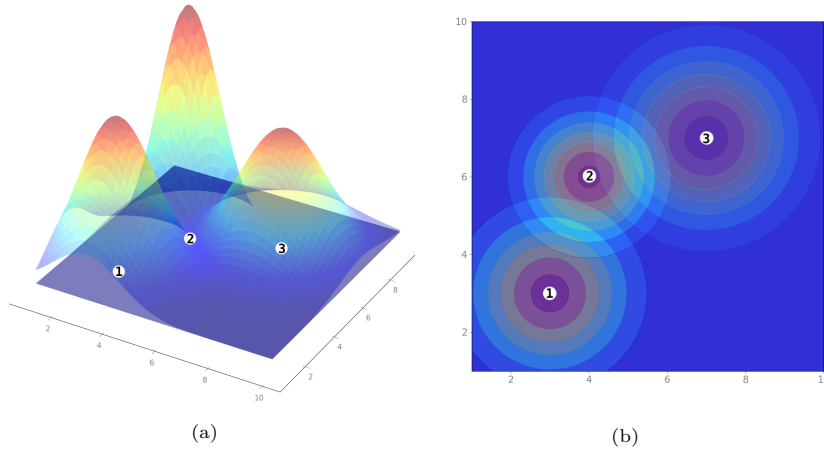


Fig. 1. Illustration of the PDF of the Gaussian distribution centered on three sample Stores : (a) 3D visualisation; (b) 2D visualisation. The white dots indicate the store location and the numbers are used to identify the respective stores on 3D and 2D visualisations.

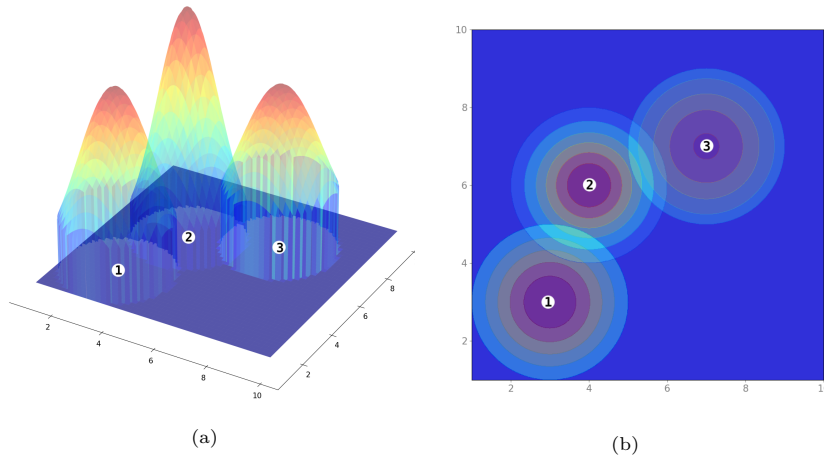


Fig. 2. Illustration of the Truncated Gaussian centered on three sample Stores: (a) 3D visualisation; (b) 2D visualisation. The white dots indicate the store location. There is a hard border around the distributions beyond which the PDF is equal to zero.

Given the truncated Gaussian distributions, we define the probability p_{ns} of a customer visiting the s -th store as:

$$p_{ns} = \frac{\mathbf{Z}_s(\mathbf{m}_n)}{\sum_{j=1}^S \mathbf{Z}_j(\mathbf{m}_n)}. \quad (4)$$

Note that we normalize the PDF calculated for the customer with respect to the store by the total PDF respect to all the stores within the consideration set to arrive

at a value which falls in the interval of $[0, 1]$. Thus we assume that every customer chooses at least one store in their consideration set, but this can be relaxed by adding pseudo stores to account for unsatisfied demand or unobserved data. The value of p_{ns} capture the level of competition in the region τ for a specific type of store. For instance, p_{ns} will be lower in competitive markets or areas while it will take higher values in non-competitive settings. This is illustrated in Fig. 3 with respect to the non-truncated and truncated Gaussian distributions.

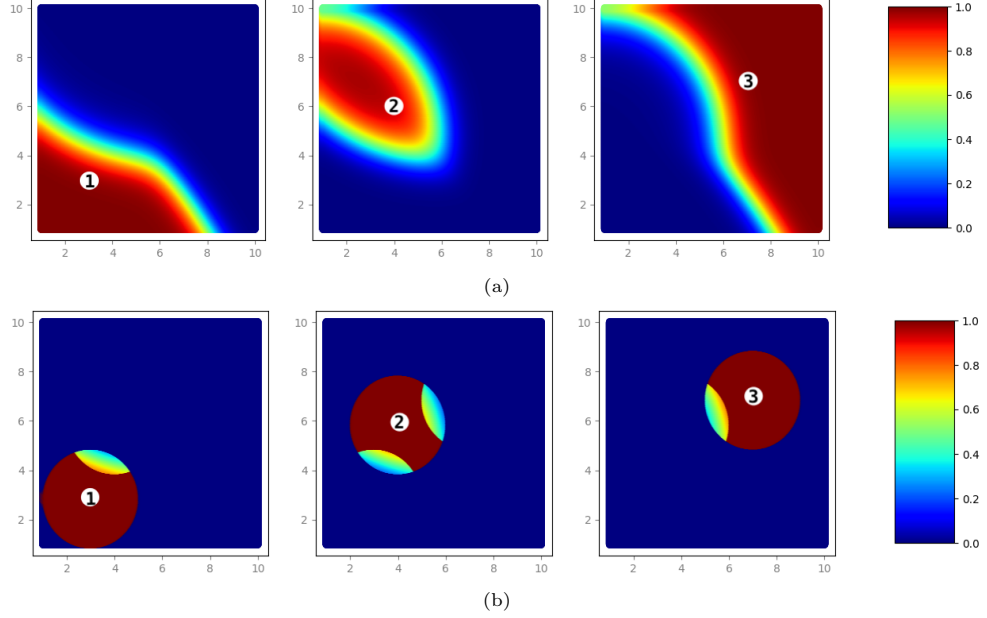


Fig. 3. Illustration of the probability of customers visiting a store p_{ns} : (a) with none truncated Gaussian distribution; (b) with truncated Gaussian distribution. This is an indication of the competition in the area. The white dots indicate the store location, and the numbers are used to identify the respective stores on (a) and (b) plots.

The consumption function in economics determines the relationship between consumer spending and the various factors (Modigliani and Brumberg, 1954). To model the amount budgeted by each customer for spending we propose a linear function $f(\cdot)$ which takes input $\mathbf{v}_n[-\mathbf{m}_n]$ representing the $P - 2$ customer features obtained by discarding the location coordinates:

$$r_n = f(\mathbf{v}_n[-\mathbf{m}_n]) = \boldsymbol{\beta}^T \mathbf{v}_n[-\mathbf{m}_n], \quad (5)$$

where $\boldsymbol{\beta} \in \mathbb{R}^{P-2}$. This leads to the conventional Spatial interaction system (Huff, 1963; Wilson, 1971; Ellam et al., 2018). Thus expenditure flow from customer n to store s :

$$r_{ns} = r_n \times p_{ns}, \quad (6)$$

where the amount each customer budgeted to spend r_n is weighed by the probability

to visit the s -th store. The total revenue for the s -th store is:

$$r_s = \sum_{n=1}^N r_n p_{ns} = \sum_{n=1}^N \boldsymbol{\beta}^T \mathbf{v}_n[-\mathbf{m}_n] \frac{\mathbf{Z}_s(\mathbf{m}_n)}{\sum_{j=1}^S \mathbf{Z}_j(\mathbf{m}_n)}. \quad (7)$$

Henceforth we derive the model for the case where the store variance is a function of its features (Eq. (2)), since the limiting case where the store variance is store specific coefficient (Eq. (1)) is a trivial extension by setting λ to zero.

Likelihood function: The likelihood of the observed stores' revenue $\mathbf{Y} = \{y_1, \dots, y_S\}$ is defined as:

$$p(\mathbf{Y}|\boldsymbol{\beta}, \lambda, \varepsilon, \sigma^2) = \prod_{s=1}^S \mathcal{N}(y_s; r_s, \sigma^2), \quad (8)$$

where the model assumes constant-variance (σ^2) for the Gaussian noise.

Prior Distributions: We assign prior distributions to all model parameters. First, we define a hierarchical prior distribution for $\boldsymbol{\beta}$, which we assume to be a Gaussian with mean μ_β and covariance $\alpha^{-1}\mathbf{I}$:

$$p(\boldsymbol{\beta}|\alpha) = \mathcal{N}(\boldsymbol{\beta}; \mu_\beta, \alpha^{-1}\mathbf{I}),$$

Following the standard practices, we introduce a Gamma prior distribution with shape $\omega_1 > 0$ and scale $\omega_2 > 0$ for the hyper-parameter α :

$$p(\alpha) = \text{Gam}(\alpha; \omega_1, \omega_2)$$

Similarly, we assign a Gamma prior distribution with shape ρ_1 and scale ρ_2 for the likelihood precision parameter $\gamma = \sigma^{-2}$:

$$p(\gamma) = \text{Gam}(\gamma; \rho_1, \rho_2),$$

Finally, the following Gaussian prior distributions are selected for λ and ε with mean μ and covariance $\varrho\mathbf{I}$,

$$\begin{aligned} p(\lambda) &= \mathcal{N}(\lambda; \mu_\lambda, \varrho_\lambda \mathbf{I}) \\ p(\varepsilon) &= \mathcal{N}(\varepsilon; \mu_\varepsilon, \varrho_\varepsilon \mathbf{I}). \end{aligned}$$

Posterior Distribution: The full vector of model parameters is denoted by $\boldsymbol{\Theta} = \{\boldsymbol{\beta}, \lambda, \varepsilon, \gamma\}$. Posterior probability given by:

$$p(\boldsymbol{\Theta}|\mathcal{D}) = \frac{p(\mathcal{D}|\boldsymbol{\Theta})p(\boldsymbol{\Theta})}{\int p(\mathcal{D}|\boldsymbol{\Theta})p(\boldsymbol{\Theta})d\boldsymbol{\Theta}} \quad (9)$$

where the marginal density takes the form:

$$p(\mathcal{D}) = \int \cdots \int p(\mathcal{D}|\boldsymbol{\beta}, \lambda, \gamma)p(\boldsymbol{\beta}|\alpha)p(\alpha)p(\lambda)p(\varepsilon)p(\gamma) d\boldsymbol{\beta} d\alpha d\lambda d\varepsilon d\gamma. \quad (10)$$

$$q(\alpha) = \text{Gam}(\alpha; \hat{\omega}_1, \hat{\omega}_2), \quad (13)$$

$$q(\gamma) = \text{Gam}(\gamma; \hat{\rho}_1, \hat{\rho}_2), \quad (14)$$

$$q(\lambda) = \mathcal{N}(\lambda; \hat{\mu}_\lambda, \mathbf{K}_\lambda), \quad (15)$$

$$q(\varepsilon) = \mathcal{N}(\varepsilon; \hat{\mu}_\varepsilon, \mathbf{K}_\varepsilon), \quad (16)$$

where $\boldsymbol{\nu} = \{\hat{\mu}_\beta, \boldsymbol{\Omega}, \hat{\omega}_1, \hat{\omega}_2, \hat{\rho}_1, \hat{\rho}_2, \hat{\mu}_\lambda, \mathbf{K}_\lambda, \hat{\mu}_\varepsilon, \mathbf{K}_\varepsilon\}$ are the variational parameters which are optimized within the algorithm. Eqs. (12)–(16) define our approximate posterior. With this, we give details of the variational objective function, i.e. ELBO, which we aim to maximize with respect to $\boldsymbol{\nu}$.

Evidence Lower Bound: Following the standard variational inference, ELBO can be written as a combination of expected log likelihood (\mathcal{L}_{ell}) and KL-divergence term (\mathcal{L}_{kl}):

$$\mathcal{L}_{\text{elbo}}(\boldsymbol{\nu}) = \mathcal{L}_{\text{ell}}(\boldsymbol{\nu}) - \mathcal{L}_{\text{kl}}(\boldsymbol{\nu}). \quad (17)$$

the expected log likelihood term can be written as

$$\begin{aligned} \mathcal{L}_{\text{ell}} &= \mathbb{E}_{\boldsymbol{\beta}, \gamma, \lambda, \varepsilon} [\ln p(Y | \boldsymbol{\beta}, \gamma, \lambda, \varepsilon)] \\ &= -\frac{S}{2} \ln 2\pi + \frac{S}{2} (\psi(\hat{\rho}_1) - \ln \hat{\rho}_2) - \\ &\quad \frac{1}{2} \frac{\hat{\rho}_1}{\hat{\rho}_2} \mathbb{E}_{\boldsymbol{\beta}, \gamma, \lambda, \varepsilon} \left[\frac{\gamma}{2} \sum_{s=1}^S \left(y_s - \boldsymbol{\beta}^\top \sum_{n=1}^N \mathbf{v}_n[-\mathbf{m}_n] \frac{\mathbf{Z}_s(\mathbf{m}_n)}{\sum_{j=1}^S \mathbf{Z}_j(\mathbf{m}_n)} \right)^2 \right] \end{aligned} \quad (18)$$

the KL-Divergence Term is expanded and simplified as:

$$\begin{aligned} \mathcal{L}_{\text{kl}} &= \mathbb{E}[\ln p(\boldsymbol{\Theta})] - \mathbb{E}[\ln q(\boldsymbol{\Theta})] \\ &= \mathbb{E}_{\boldsymbol{\beta}, \alpha} [\ln p(\boldsymbol{\beta} | \alpha)] + \mathbb{E}_\alpha [\ln p(\alpha)] + \mathbb{E}_\lambda [\ln p(\lambda)] + \mathbb{E}_\varepsilon [\ln p(\varepsilon)] + \mathbb{E}_\gamma [\ln p(\gamma)] - \\ &\quad \mathbb{E}_{\boldsymbol{\beta}} [\ln q(\boldsymbol{\beta})] - \mathbb{E}_\alpha [\ln q(\alpha)] - \mathbb{E}_\lambda [\ln q(\lambda)] - \mathbb{E}_\varepsilon [\ln q(\varepsilon)] - \mathbb{E}_\gamma [\ln q(\gamma)], \end{aligned} \quad (19)$$

where each term is given in the Appendix A. $\mathcal{L}_{\text{elbo}}(\boldsymbol{\nu})$ is not computable in analytically closed forms and remains intractable. Hence we resort to Black Box variational inference method where the gradient is computed from the Monte Carlo samples from the variational distributions (Ranganath et al., 2014). We implement the algorithm using Tensorflow 2 (Abadi et al., 2016) in Python 3.

2.2.2. Markov Chain Monte Carlo

In order to compare our estimations we describe the MCMC which has been the dominant paradigm for approximate inference for decades. First, we construct a Markov chain on $\boldsymbol{\Theta}$ whose stationary distribution is the posterior $p(\boldsymbol{\Theta} | \mathcal{D})$. Then we collect samples from the stationary distribution by sampling from the Markov chain. Finally, we use the collected samples to approximate the posterior with an empirical estimate. MCMC methods ensure producing exact samples from the target density but tend to be computationally intensive (Robert and Casella, 2013). When the datasets are large, MCMC becomes slower and computationally expensive to form

inferences. We use open-source software, Stan which is a C++ library for Bayesian modeling, with the R interface to compile results (Stan Development Team, 2020). We adopt the No-U-Turn sampling method, an extension to Hamiltonian Monte Carlo algorithm for the experiments (Hoffman et al., 2014).

2.3. Edge Correction

Stores on the edge of the study area τ cannot be evaluated without a certain bias because the model cannot capture the contribution from customers living outside τ . To overcome this, we adjust the revenues of the stores $\{y_s\}_{s=1}^S$, and this is carried out before fitting the model. Following a similar approach to the model, we assume a Gaussian centered on the store and calculate the area under the curve (AUC) \mathcal{A} , which intersects with the study area. We set the variance η^2 of the Gaussian to be $d_T/4$ to cover approximately an area of 0.99 within the buffer radius of d_T around the store center \mathbf{l}_s . Calculating the AUC for an arbitrary polygon as shown in Fig. 5, is computationally challenging. Henceforth we use the Monte Carlo method, where the samples are drawn from $\mathcal{N}(\mathbf{l}_s, \eta^2 \mathbf{I})$ and reject them if outside the τ to calculate the fraction of kept samples.

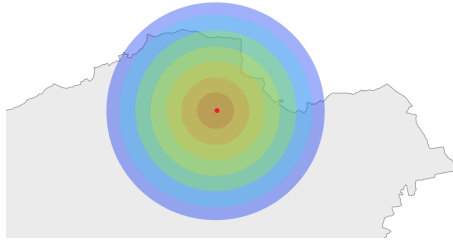


Fig. 5. The red marker denotes a store at the edge of London. There may be customers who contributes to its revenue but not in the study area. Intersection of the radius and London map results in an arbitrary polygon shape.

We formulate the adjusted revenue \tilde{y}_s as the actual revenue weighted by the AUC:

$$\tilde{y}_s = y_s \times \mathcal{A}. \quad (20)$$

We apply this to real-world data for edge correction before fitting the BSIM.

3. Simulation study

We design a simulation study to examine the inferences obtained from VI and MCMC methods under different synthetic settings characterised by an increasing number of stores and customers. We also compare the computational performance of the two methods by observing the run time of each fitted model. First, we simulate the data from a spatial process that closely matches the modeling framework introduced in Section 2, Eq. (2) with $\varepsilon_s = 0$. The process is defined as:

$$y_s | \boldsymbol{\beta}, \boldsymbol{\lambda}, \sigma^2 \sim \mathcal{N}(r_s, \sigma^2), \quad (21)$$

Table 1. The first row indicates the True values of the parameters used to create the synthetic data, and the following rows display the first (Mean) and second moments (Standard deviation) along with its 95% quantile-based Credible Intervals (CI) for the posterior distributions for VI and MCMC methods.

		β_1	β_2	λ_1	λ_2	γ
True		-0.2	0.4	0.1	0.5	4
VI	Mean	-0.196	0.398	0.164	0.383	1.821
	Std	0.014	0.018	0.235	0.116	0.727
	CI	(-0.224, -0.169)	(0.362, 0.434)	(-0.296, 0.625)	(0.156, 0.609)	(0.687, 3.499)
MCMC	Mean	-0.198	0.400	0.185	0.387	1.908
	Std	0.017	0.021	0.547	0.393	0.904
	CI	(-0.235, -0.166)	(0.358, 0.447)	(-0.839, 1.387)	(-0.313, 1.269)	(0.562, 4.054)

where the locations of stores and customers are simulated within a square. Two customer features are generated, one with a strong spatial correlation and the other with a moderate spatial correlation to closely reflect the real-world customer features as shown in Fig. 6. The store locations are randomly sampled within the same spatial boundaries used to sample the customers. Store features are sampled from a Gamma distribution ($\Phi \sim \text{Gam}(1, 1)$) to represent features such as floorspace.

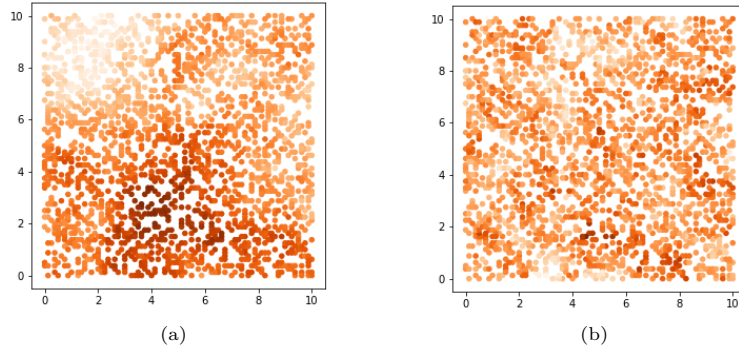
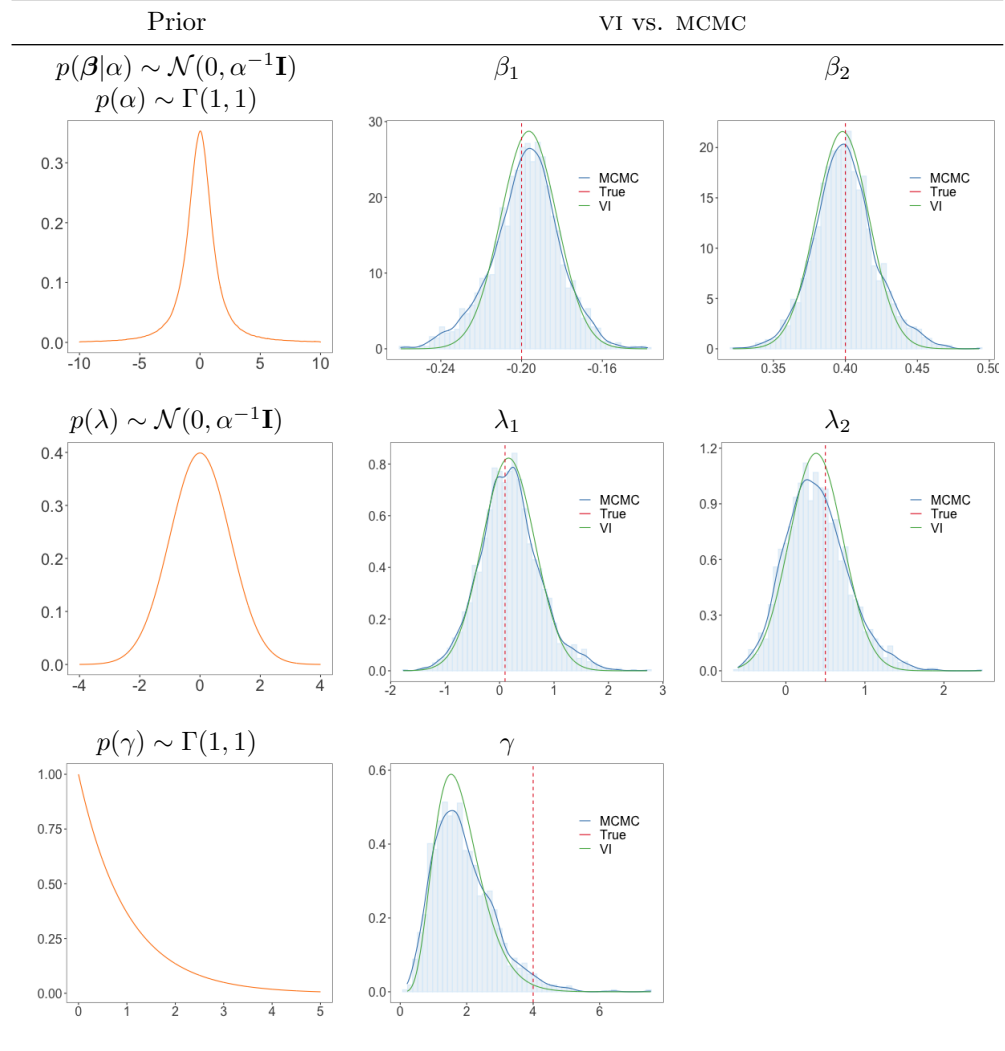


Fig. 6. Simulated Customer features for $N = 1000$ under two different spatial correlation structures to closely simulate the real-world scenarios: (a) Strong Spatial Correlation; (b) Moderate Spatial Correlation.

3.1. Parameter Estimation

For both VI and MCMC methods, all priors are chosen to be weakly informative to allow the data to drive the inference as illustrated in Table 2. We fit our MCMC model using one chain with 5000 iterations by removing the first 2500 for warm-up, and every post-warm-up iteration is used for posterior samples. The posterior distributions along with the prior distributions are visualised in Table 2 and parameter estimates are presented in Table 1. The results indicate that both methods approximate the posterior mean effectively and variational approximations of the posterior variance are lower than MCMC method.

Table 2. Column one demonstrates the weakly informative prior distributions, and the following columns illustrate marginal posteriors of the interested parameters inferred by VI and MCMC. Synthetic experiment consists of 10 stores and 1000 customers ($S = 10, N = 1000$).



The simulation process explained above is experimented under two different synthetic settings:

- (a) sim_1 : 10 stores with 1000 individuals ($S = 10, N = 1000$)
- (b) sim_2 : 50 stores with 2000 individuals ($S = 50, N = 2000$)

We simulate random store locations to create 50 datasets and compare the performance across datasets using the posterior means of β, λ, γ and the 95% quantile-based credible intervals for each parameter from each fitted model. Three standard measures are used to compare the performance between MCMC and VI methods:

- (a) the bias, which measures the differences between the posterior mean from the model fit to dataset $_i$ ($\hat{\beta}_i$) and the true value of the parameter β , $\text{Bias} = \frac{1}{50} \sum_{i=1}^{50} (\hat{\beta}_i - \beta)$;
- (b) the mean-squared error (MSE), which takes the squared of the difference between posterior mean and true value, $\text{MSE} = \frac{1}{50} \sum_{i=1}^{50} (\hat{\beta}_i - \beta)^2$;
- (c) the coverage of the 95% quantile-based credible interval obtained from fitting the model to dataset $_i$, $\text{coverage} = \frac{1}{50} \sum_{i=1}^{50} I(\beta \in \text{credible interval}_i)$, where $I(\cdot)$ is the indicator function equal to 1 if the statement is true and 0 otherwise.

Table 3 and Table 4 show the results of the fitted models for the two synthetic settings, averaged across the 50 datasets. Both VI and MCMC algorithms exhibit comparable performance in terms of bias, MSE, and coverage across both simulation studies. For sim_1 , we observe lower coverage for γ with the VI scheme. However the coverage for γ is improved to one in the sim_2 . Both λ and γ parameters result in a higher estimated MSE under both the simulation setting for VI and MCMC methods. This is an indication of the lack of identifiability in the parameters due to the flexibility in the model. The precision γ of the error term σ^2 tends to be underestimated on average. Both models are fitted on a Intel Xeon CPU (3.5GHz and 32 GB of RAM). The run time of the VI algorithm is about five times faster than the MCMC algorithm in the simulation study. This is vital for our real-world data application, where the number of spatial locations is much larger than the synthetic settings. Overall the VI algorithm exhibited a reduced run time while providing good estimations and inference of the parameters of interest in this simulation study.

3.2. Model Comparison

Finally under the simulation study, we conduct a comparison of our model with the Huff modified model (Li and Liu, 2012). Two standard metrics are used to evaluate the performance:

- (a) the Normalised Root-Mean-Squared Error (NRMSE), which measures the differences between the values predicted by a model ($\hat{\mathbf{Y}}$) and the values observed (\mathbf{Y}), $\text{NRMSE} = \frac{\sqrt{E[\mathbf{Y} - \hat{\mathbf{Y}}]^2}}{E[\mathbf{Y}]}$;

Table 3. VI and MCMC simulation study performance for $S = 10, N = 1000$.

Metric	Method	β_1	β_2	λ_1	λ_2	γ
Bias	VI	-0.002	0.004	0.258	0.110	-1.828
	MCMC	-0.002	0.004	0.265	0.116	-1.772
MSE	VI	0.000	0.000	0.130	0.051	3.467
	MCMC	0.000	0.42	0.130	0.049	3.276
Coverage	VI	0.94	0.96	1.	1.	0.44
	MCMC	0.96	0.98	1.	1.	0.94
Run time (s)		VI 207		MCMC 1064		

Table 4. VI and MCMC simulation study performance for $S = 50, N = 2000$.

Metric	Method	β_1	β_2	λ_1	λ_2	γ
Bias	VI	0.000	0.002	-0.338	0.352	-0.754
	MCMC	0.002	-0.001	-0.092	0.341	-0.734
MSE	VI	0.000	0.000	0.185	0.179	0.598
	MCMC	0.000	0.000	0.008	0.186	0.571
Coverage	VI	1.	0.94	0.84	0.94	1.
	MCMC	1.	1.	1.	0.857	1.
Run time (s)		VI 1079		MCMC 5280		

- (b) the R-squared, which is the ratio of the variance of the residuals (SS_{res}) and the variance of the observed \mathbf{Y} (SS_{tot}), $R^2 = 1 - \frac{SS_{res}}{SS_{tot}}$.

Table 5 displays the results for BSIM and Huff modified model. BSIM exhibits better performance across both the settings compared to the modified Huff model. We observe an increase in NRMSE for both models as the number of stores and customers increases. However, the R^2 remains unaffected at significantly high levels showing more robust performance for BSIM under both simulation settings compared to the modified Huff model.

Table 5. Performance of the simulation studies for BSIM and Huff modified model. $sim_1 : S = 10, N = 1000$ and $sim_2 : S = 50, N = 2000$.

		sim_1	sim_2
R^2	Model	0.98	0.94
	Modified Huff Model	0.77	0.30
NRMSE	Model	0.07	0.15
	Modified Huff Model	0.24	0.64

4. Large-scale geospatial dataset of pub activities in London

We initially develop a large-scale, geospatial dataset for England non-domestic properties using data from multiple sources. However, for the interest of this study, we limit to one non-domestic property category, public houses (pubs), which are located in Greater London. To the best of our knowledge, this is the first study exploring these datasets together to benefit retail businesses. A detailed description of each dataset is given in Appendix B. All the spatial data processing is done using PostGIS on a PostgreSQL database.

4.1. Store level data

We compile a dataset with stores' geospatial location, rateable values, and store-specific features. We do this by Joining the VOA (Valuation Office Agency, 2019) and Addressbase from Ordnance Survey (2019) data using the cross-reference which renders all of the non-domestic properties geo-coordinates and their rateable values. The calculation of the rateable values of pubs is different from other categories. In contrast, the rateable value of pubs is based on the annual level of trade (excluding VAT) that a pub is expected to gain if operated in a reasonably efficient way (Valuation Office Agency, 2016). Hence the rateable value is a good proxy of the pub revenues, and we use data related to pubs for the real-world experiment in this study. There are 40,000 pubs recorded in VOA for England and Wales. The spatial distribution of pubs across England is shown in Fig. 7.

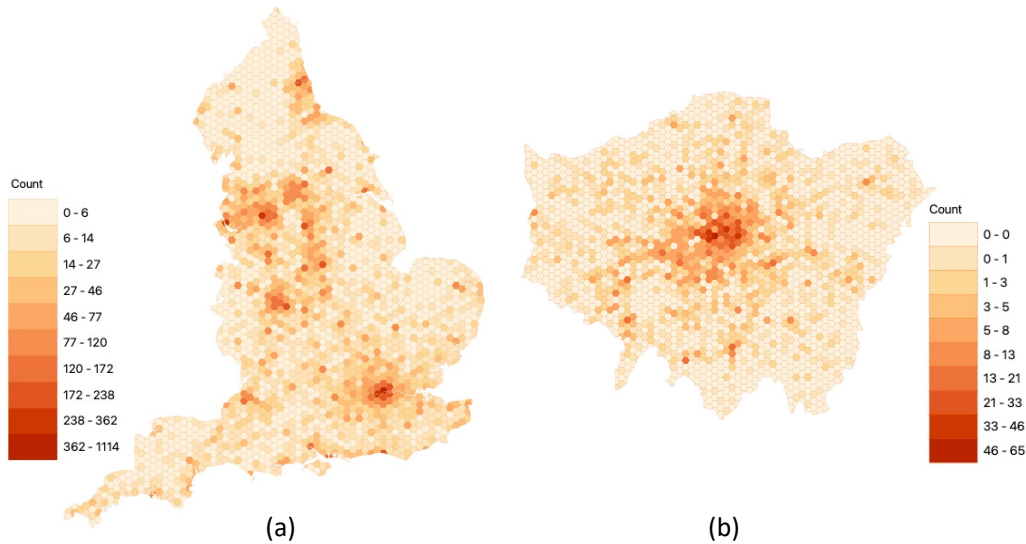


Fig. 7. Spatial distribution of pubs: (a) across England; (b) zoomed into Greater London. The region is split into equal size grids of hexagons (size of each side : (a) 5km; (b) 0.5km) and number of pubs within each hexagon is displayed with a colour gradient.

The store features are an essential factor in assessing the attractiveness of the stores. The internal store characteristics of the building, such as the floor size, height are extracted from the OS Mastermaps from Ordnance Survey (2020). This is accomplished by first spatially joining the polygon of the land (HM Land Registry, 2020) with locations of stores and next spatially join the polygon of the footprint from Mastermaps. Additionally, external characteristics such as the closest distance to public transport access points (Department for Transport, 2014), tourist attractions (Historic England, 2014) are calculated using the Euclidean distance between spatial locations. We have strengthened the store attractiveness measures by using the customer reviews on Google (Google, 2020). People can write reviews and rate the places voluntarily on Google maps. The ratings are then aggregated and shown to the public. Using the Google Places API, this data can be accessed at a cost. Flow diagram of the process used to extract the store features are demonstrated in Fig. 8.

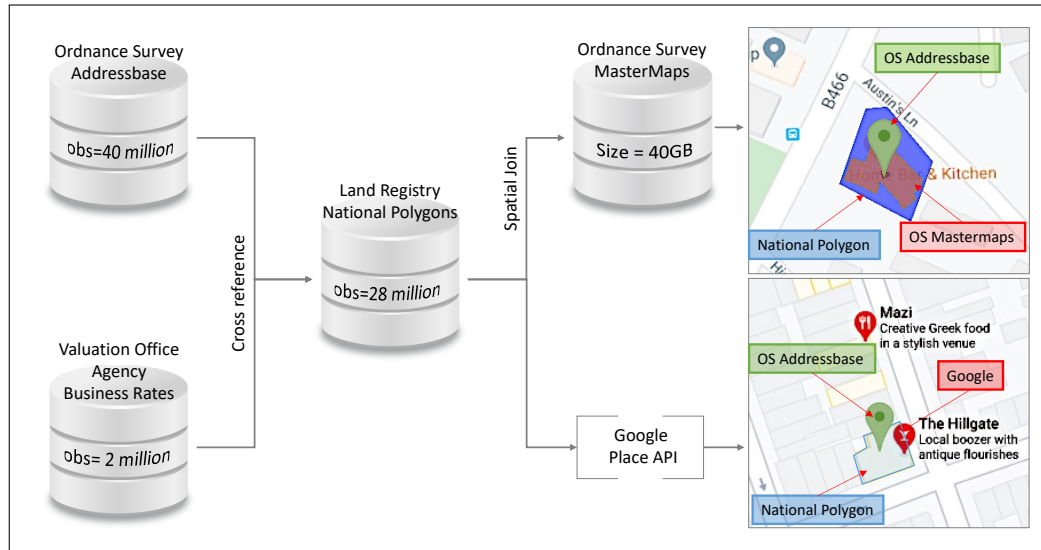


Fig. 8. Diagram illustrates the steps to extract the store features. Each dataset is named as per the data source along with its number of records (obs) or size. Initially OS addressbase is joined with VOA dataset and then spatially joined with National Polygons data to find the Title polygon of each land. This is next joined with Mastermaps and linked with Google data to obtain the store footprints and google customer ratings respectively.

4.1.1. Customer level data

The most granular level of customer data can be identified as the residential locations. OS Addressbase dataset provides both residential and commercial addresses (over 40 million) along with geo-locations. However, since there is no data for customer features at the residential level, in this study, we use postcodes which is the next most granular level. Henceforth, we assume that the customers' behaviour who are residing in the same postcode are homogeneous. In Greater London on average there are 17 households per postcode. The postcode centroids for Greater London

are displayed in Fig. 9. The population and proportion of gender at the postcode level are used to reflect the demographics in the area. Additionally, we employ the deprivation data to understand the customer characteristics in the area (Ministry of Housing, Communities & Local Government, 2019). There are seven domains of deprivation categories: (1) Income Deprivation, (2) Employment Deprivation, (3) Education, Skills and Training Deprivation, (4) Health Deprivation and Disability, (5) Crime, (6) Barriers to Housing and Services and (7) Living Environment Deprivation. Deprivation level data is provided at the LSOA level. We assign that to the postcodes by point to polygon spatial join.

5. Case study: estimating revenues of pubs in London

In this section, we illustrate our proposed methodology using the pubs’ dataset developed for Greater London in section 4. After compiling data from different sources, the final complete dataset consists of $S = 1804$ pubs. The derived approximated revenue after adjusting for edge correction (Eq. (20)) is used as the response variable y_s in the model with natural log transformation. For each pub, we derived pub-specific features: floorspace, height, number of floors, the total area of land; distance to the closest metro, train station, bus stop, park, popular attractions, sports facility; customer rating on Google, number of users rated and an indicator to show if the pub is in a major town.

We determine the customer locations at the postcode level, which is the most granular level of census estimates are released. There are $N = 174360$ postcodes for Greater London. We represent the characteristics of the postcodes by the population at each postcode and its proportion of male, and deprivation scores. All features have been normalized before training the model. The model may be improved with more granular customer-specific characteristics; underlying arguments would remain the same. Centroids of the postcodes and retail locations of the pubs are presented in Fig. 9(a), on a map of London.

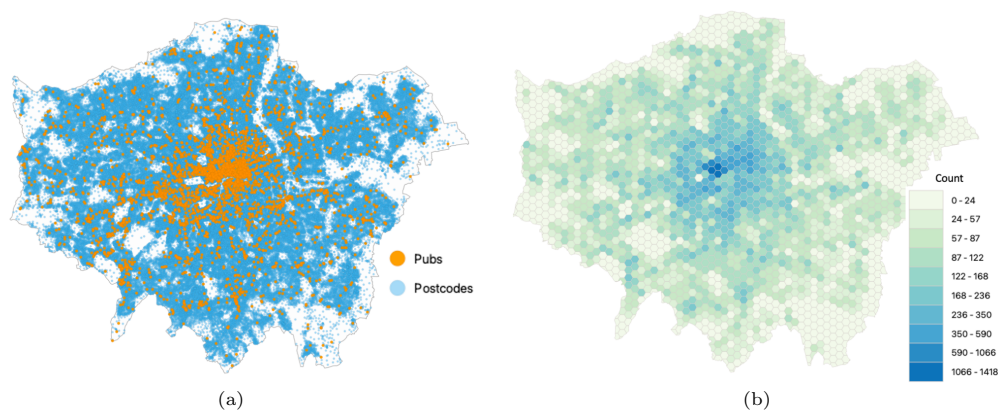


Fig. 9. (a) Visualization of the locations of pubs in orange markers ($S = 1804$) and postcode centroids in blue markers ($N = 174360$) over the map of London; (b) Greater London is split into equal size grids of hexagons (size of each side is 0.5km) and number of postcodes within each hexagon is displayed with a colour gradient.

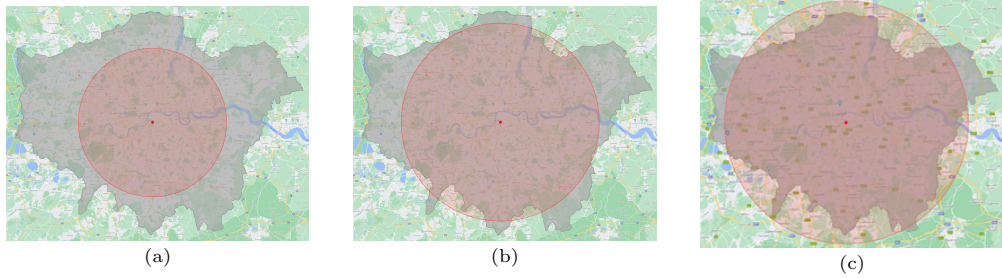


Fig. 10. Demonstration of different radius used for truncated Gaussian with an example concerning a pub located in the center of London. Three radii were used in the study: (a) 15km; (b) 20km; (c) 25km.

Table 6. R^2 , σ^2 and NRMSE for the fitted BSIM with revenues of pubs in Greater London under three different radii of the truncated Gaussian.

	Truncated radius (km)		
	15	20	25
R^2	0.19	0.72	0.57
σ^2	0.67	0.45	0.52
NRMSE	0.08	0.05	0.06

Customer behavior is not affected after a certain distance from the business facility, despite the pubs' attractiveness. We explore the model under three different radius, $d_T = 15\text{km}$, 20km and 25km as presented in Fig. 10. We calculate the distance between origin and pub using Euclidean distance, although a better representation would use a transport network.

We first perform a preliminary study of our model with a store-specific coefficient which denotes the store-specific variance $\sigma_s^2 = \exp(v_s)$, representing the attractiveness of the store as given by Eq. (1). We experiment with the model for three different radii of the truncated Gaussian and model performance summarised in Table 6. Results indicate that R^2 increased to 0.72 as the radius increased from 15km to 20km but reduced to 0.57 as the radius increased to 25km. Hence the best experimental results yielded for truncated Gaussian with a radius of 20km.

Next, we perform a detailed study on the model with improved specifications where store features represent the attractiveness of the store (Eq. (2)). In this study, the radius of the truncated Gaussian is set to 20km, as it demonstrated the best results for the previous experiment. The model with these settings resulted in a high R^2 of 0.88 and a low NRMSE of 0.03. The plots (Fig. 11) of the observed revenue and predicted revenues suggest that the model provides a good fit to the data. The residuals are relatively high out of central London, closer to a major ringway as shown in Fig. 11 c. Additionally, the predicted revenue of a few pubs at the edge of the study area is underestimated, reflecting the edge effects.

Using the parameter estimates (λ, ε) from the best-fitted model, we have demon-

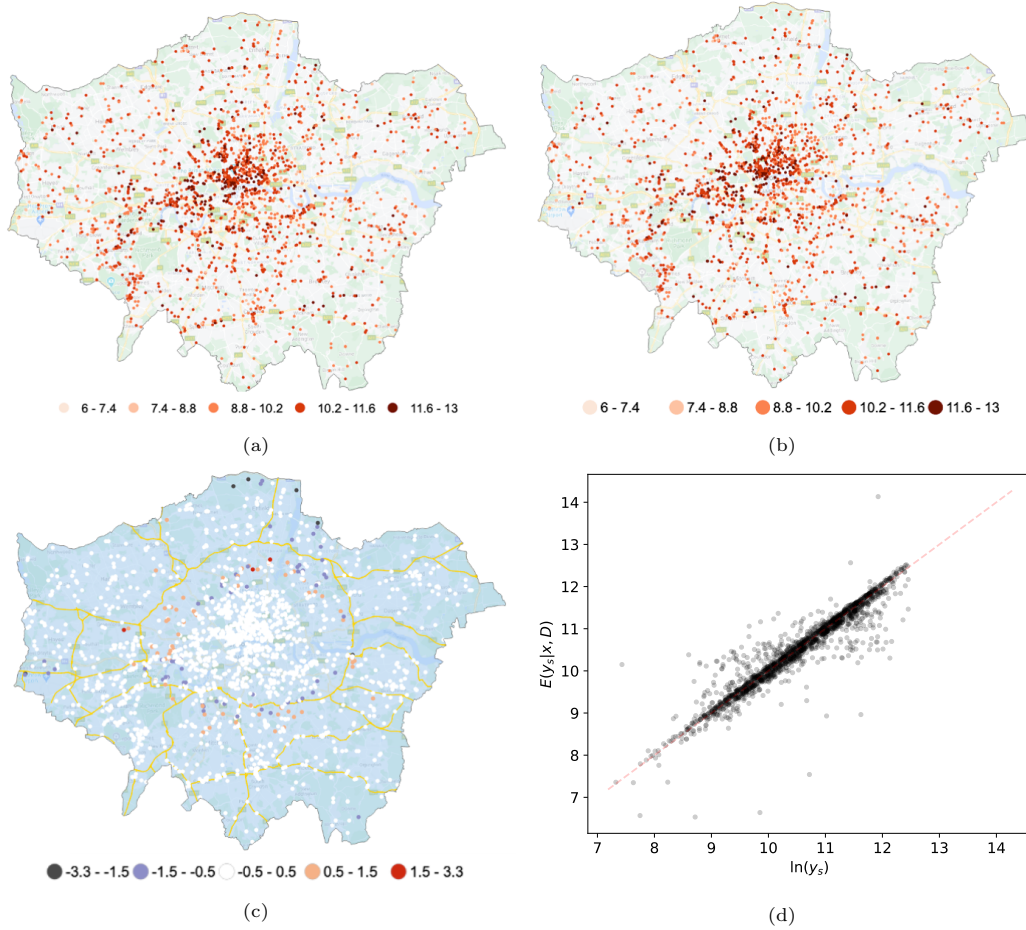


Fig. 11. Visualisation of the Pub’s revenue and predictions over greater London map with truncated Gaussian radius of 20 km: (a) Revenue at each pub; (b) Predicted revenue at each pub; (c) Residuals marked in points and lines are the major roads; (d) Actual against predicted revenue. The experiment resulted in $R^2 = 0.88$ and $NRMSE = 0.03$.

strated the attractiveness (σ_s^2) of pubs around London in Fig. 12(a). It can be observed that the most attractive pubs are within or around the major towns. Further exploring the coefficients of pub features, we found that Google’s customer rating score and the number of people rated had the highest positive contribution towards the attraction term (Appendix C). This implies that customer rating is a critical indicator in describing the customer attractiveness to the pubs. The remaining term used to express the attractiveness, unobserved pub features (ε_s), where the absolute coefficient is mapped in Fig. 12(b). There is a similar pattern to the residual plot, but overall spatial distribution appears to be random. A deep investigation is required to understand what could explain the unobserved pub features.

For demonstration purposes, we randomly select a pub in central London to explore the insights from the fitted model. The probability of people within the

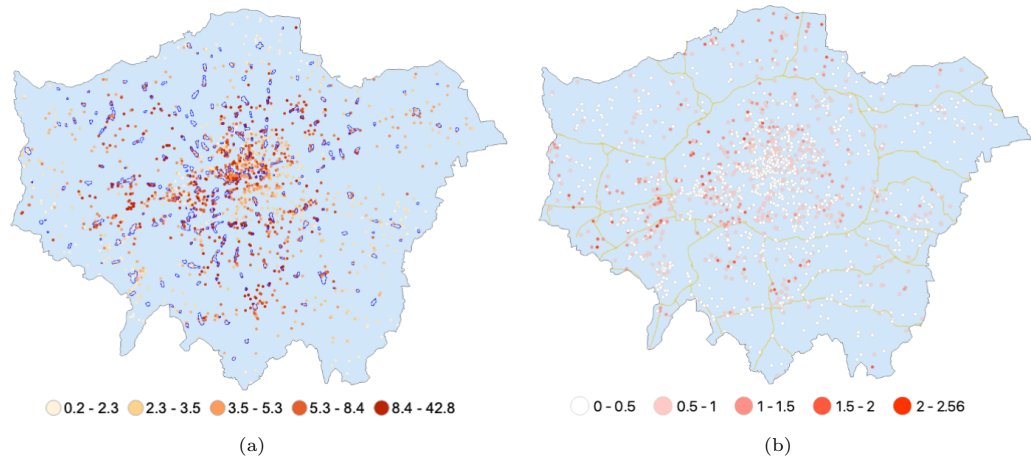


Fig. 12. Exploring the pubs attractiveness for the fitted model: (a) Variance (σ_s^2) of the Gaussian placed on each pub. Blue colour polygons denote the major towns; (b) Absolute coefficients of the unobserved pub characteristics (ε_s).

postcode selecting the particular pub (p_{ns}) is calculated using the model parameter estimates with Eq. (4). These probabilities are mapped into a heatmap as shown in Fig. 13. There appear to be two hotspots on the map, one closer to the pub, and another one towards North-West London. It is natural to see higher probabilities closer to the pub, but the other hotspot is possible because the pubs' density in the area is comparatively low, as shown in Fig. 9(a). Hence people in the area also prefer traveling to pubs in central London. The distribution of probabilities tends to be having an oval shape, possibly because the distance between the customers and pubs is calculated as Euclidean distance. A better representation could occur in using a transport network.

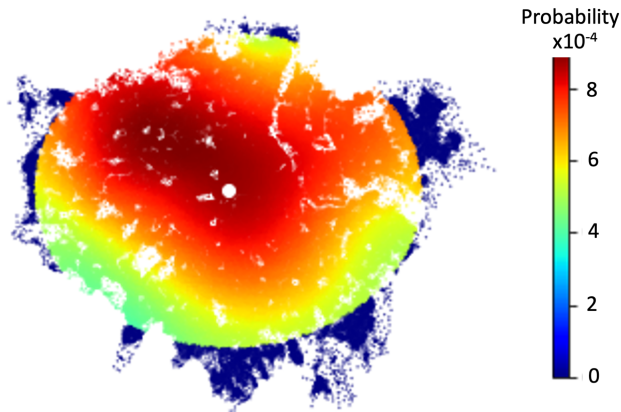


Fig. 13. Visualisation of the probability (p_{ns}) of people in each postcode selecting the particular pub shown in a white dot in the centre of London.

Using the parameter estimates (β) from the best-fitted model, we can estimate the amount spent by customers living in each postcode (r_n). Coefficients of the deprivation features indicate that areas with higher income, high employment, less risk of crimes, better quality of life, and environment tend to positively influence the customers' spending levels at pubs. The amount spent at each Borough can be derived by calculating the total of the estimated spending amount at each postcode within the Borough. This we compare against the alcohol-related mortality in the London Boroughs published by Public Health England (2021). The rank of Boroughs respective to the spending and mortality levels published for 2017 is mapped in Fig. 14. The rank correlation between mortality count and estimated spending shows a moderate positive relationship of 0.4. Our intuition is that higher alcohol-related mortalities are to be expected in the areas of high alcohol consumption.

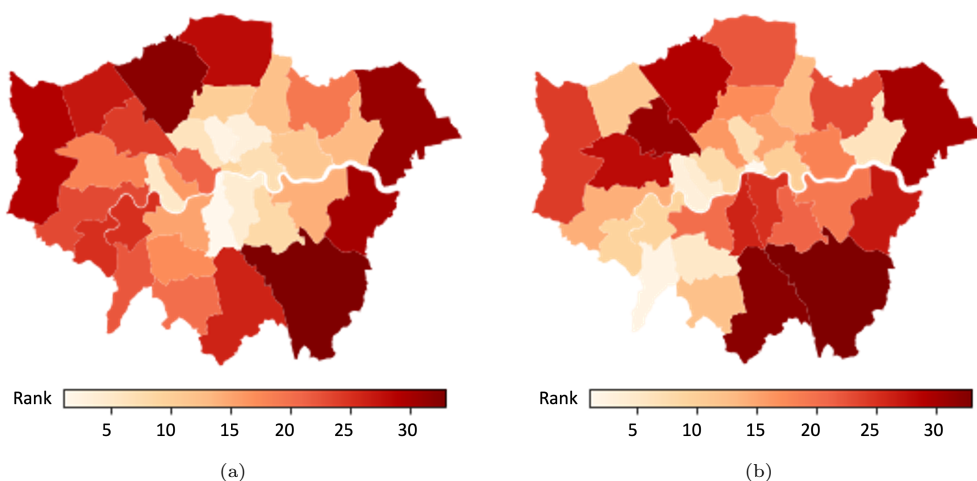


Fig. 14. Visualisation of ranking on estimated revenue and mortality in the London Boroughs : (a) Rank of estimated amount spent at the pubs by people living in each Borough; (b) Rank of Mortality count.

Finally, we perform a comparison with a spatial interaction model from the literature for completeness of the study. We fitted the Modified Huff model (Li and Liu, 2012) for the same dataset, which displayed very low performance with R^2 of only 0.03 and NRMSE of 0.84. Our model outperforms the benchmark model with a notable improvement and provides valuable inferences for decision-makers.

6. Discussion

We have developed a Bayesian spatial interaction model to simulate customers' behavior with business facilities using their respective characteristics. BSIM considerably improves existing classical Huff type models as it formally addresses uncertainties arising in the modelling process, via a Bayesian framework while providing inferences at the level of business and customer locations. The key advantage of the proposed model is scalable and can make inference on large-scale datasets through

deterministic variational inference, in contrast to the existing models. The synthetic experiments show how VI performs five times faster than MCMC while providing comparable performances in terms of parameter identification and without significant under estimation of the posterior covariance.

For the first time, we are able to demonstrate and estimate spatial interactions in large real-world urban extend such as Greater London with more than 1500 pubs and 150000 customer regions. For this purpose, we develop a large dataset at the most granular level by utilising data from multiple sources. We presented our methodology in the context of Pubs, but this can be applied in other retail businesses or even expand into sectors such as healthcare and energy. Furthermore, we demonstrate that BSIM can infer different components of the spatial interactions, thereby making valuable conclusions for a businesses' ability to make decisions. Finally, we have shown how BSIM outperforms competing approaches in terms of prediction performances while providing consistent results with related indicators observed for the London region.

The proposed methodology can be extended and improved upon across multiple dimensions. First, one could consider adopting a travel network to estimate the distance instead of the Euclidean metric used in this study (Lafferty et al., 2005; Grigoryan, 2009; Crosby et al., 2018). This could provide a more realistic configuration of the geographical setting and lead to better inferences. Furthermore, extending the proposed framework to a spatio-temporal setting to capture the time evolution of parameters to understand the behavioural changes of customers and changes in urban systems will also be of significant interest. Lastly, our work opens up the potential to utilise the BSIM to select the optimal business location.

7. Acknowledgements

We would like to thank the UK Engineering and Physical Sciences Research Council (EPSRC grant no. EP/L016710/1 and EP/R512229/1). Furthermore, this work was supported by the Alan Turing Institute under EPSRC grant EP/N510129/1, UKRI Turing AI fellowship EP/V02678X/1, and the Lloyds Register Foundation. We are also grateful to Nimbus property system limited for their support and giving access to a comprehensive property database, and for the valuable insights shared by its Director, Paul Davis.

References

- Abadi, M., Agarwal, A., Barham, P., Brevdo, E., Chen, Z., Citro, C., Corrado, G. S., Davis, A., Dean, J., Devin, M. et al. (2016) Tensorflow: Large-scale machine learning on heterogeneous distributed systems. *arXiv preprint arXiv:1603.04467*.
- Aboolian, R., Berman, O. and Krass, D. (2007) Competitive facility location model with concave demand. *European Journal of Operational Research*, **181**, 598–619.
- Bekti, R., Pratiwi, N. and Jatipaningrum, M. (2018) Multiplicative competition interaction model to obtained retail consumer choice based on spatial analysis. In

IOP Conference Series: Earth and Environmental Science, vol. 187, 012041. IOP Publishing.

- Berman, O. and Krass, D. (2002) Locating multiple competitive facilities: spatial interaction models with variable expenditures. *Annals of Operations Research*, **111**, 197–225.
- Bishop, C. (2006) *Pattern Recognition and Machine Learning*. Information Science and Statistics. Springer.
- Blei, D. M., Kucukelbir, A. and McAuliffe, J. D. (2017) Variational inference: A review for statisticians. *Journal of the American statistical Association*, **112**, 859–877.
- Congdon, P. (2010) Random-effects models for migration attractivity and retentivity: a bayesian methodology. *Journal of the Royal Statistical Society: Series A (Statistics in Society)*, **173**, 755–774.
- Crosby, H., Damoulas, T., Caton, A., Davis, P., Porto de Albuquerque, J. and Jarvis, S. A. (2018) Road distance and travel time for an improved house price kriging predictor. *Geo-Spatial Information Science*, **21**, 185–194.
- De Giovanni, L. and Tadei, R. (2014) Modeling the retail system competition. *Procedia-Social and Behavioral Sciences*, **108**, 285–295.
- Department for Transport (2014) National Public Transport Access Nodes (NaPTAN). URL: <https://data.gov.uk/dataset/ff93ffc1-6656-47d8-9155-85ea0b8f2251/national-public-transport-access-nodes-naptan>.
- Drezner, T. (2006) Derived attractiveness of shopping malls. *IMA Journal of Management Mathematics*, **17**, 349–358.
- Ellam, L., Girolami, M., Pavliotis, G. A. and Wilson, A. (2018) Stochastic modelling of urban structure. *Proceedings of the Royal Society A: Mathematical, Physical and Engineering Sciences*, **474**, 20170700.
- Fotheringham, A. S. (1983) A new set of spatial-interaction models: the theory of competing destinations. *Environment and Planning A: Economy and Space*, **15**, 15–36.
- Fotheringham, A. S. and Webber, M. J. (1980) Spatial structure and the parameters of spatial interaction models. *Geographical Analysis*, **12**, 33–46.
- Google (2020) Place Search. URL: <https://developers.google.com/places/web-service/search>.
- Grigoryan, A. (2009) *Heat kernel and analysis on manifolds*, vol. 47. American Mathematical Soc.
- Hastings, W. K. (1970) Monte carlo sampling methods using markov chains and their applications.

- Historic England (2014) Listing. URL: <https://historicengland.org.uk/listing/the-list/>.
- HM Land Registry (2020) National polygon service. URL: <https://www.gov.uk/guidance/national-polygon-service>.
- Hoffman, M. D., Gelman, A. et al. (2014) The no-u-turn sampler: adaptively setting path lengths in hamiltonian monte carlo. *J. Mach. Learn. Res.*, **15**, 1593–1623.
- Huff, D. L. (1963) A Probabilistic Analysis of Shopping Center Trade Areas. *Land Economics*, **39**, 81.
- Jordan, M. I., Ghahramani, Z., Jaakkola, T. S. and Saul, L. K. (1999) An introduction to variational methods for graphical models. *Machine learning*, **37**, 183–233.
- Lafferty, J., Lebanon, G. and Jaakkola, T. (2005) Diffusion kernels on statistical manifolds. *Journal of Machine Learning Research*, **6**.
- LeSage, J. P. and Fischer, M. M. (2008) Spatial econometric methods for modeling origin-destination flows. In *Handbook of applied spatial analysis*, 409–433. Springer.
- Li, Y. and Liu, L. (2012) Assessing the impact of retail location on store performance: A comparison of wal-mart and kmart stores in cincinnati. *Applied Geography*, **32**, 591–600.
- Ministry of Housing, Communities & Local Government (2019) English indices of deprivation 2019. URL: <https://www.gov.uk/government/statistics/english-indices-of-deprivation-2019>.
- Modigliani, F. and Brumberg, R. (1954) Utility analysis and the consumption function: An interpretation of cross-section data. *Franco Modigliani*, **1**, 388–436.
- Nakanishi, M. and Cooper, L. G. (1974) Parameter estimation for a multiplicative competitive interaction model—least squares approach. *Journal of marketing research*, **11**, 303–311.
- ONS (2020) Retail sales index internet sales. URL: <https://www.ons.gov.uk/businessindustryandtrade/retailindustry/datasets/retailsalesindexinternetsales>.
- Ordnance Survey (2019) AddressBase Premium. URL: <https://www.ordnancesurvey.co.uk/business-government/products/addressbase-premium>.
- (2020) Os mastermap topography layer. URL: <https://www.ordnancesurvey.co.uk/business-government/products/mastermap-topography>.
- Public Health England (2021) Local alcohol profiles for england. URL: <https://fingertips.phe.org.uk/profile/local-alcohol-profiles/>.
- Ranganath, R., Gerrish, S. and Blei, D. (2014) Black box variational inference. In *Artificial Intelligence and Statistics*, 814–822. PMLR.

- Reilly, W. J. et al. (1929) Methods for the study of retail relationships.
- Robert, C. and Casella, G. (2013) *Monte Carlo statistical methods*. Springer Science & Business Media.
- Stan Development Team (2020) RStan: the R interface to Stan. URL: <http://mc-stan.org/>. R package version 2.21.2.
- Valuation Office Agency (2016) Valuation of public houses 2017. *Tech. Rep. Oct.* URL: <https://www.gov.uk/government/publications/valuation-of-public-houses>.
- (2019) Business rates. URL: <https://www.gov.uk/introduction-to-business-rates>.
- Wilson, A. (2010) Entropy in urban and regional modelling: Retrospect and prospect. *Geographical Analysis*, **42**, 364–394.
- Wilson, A. G. (1971) A family of spatial interaction models, and associated developments. *Environment and Planning A*, **3**, 1–32.